Synthesis and Structural Study by Wide-Angle X-ray Scattering (WAXS) of Polymeric $\{Ln_2[M(opba)]_3\}\cdot S$ Compounds Containing 4f Ln^{III} and 3d M^{II} $\{Ln_2[M(opba)]_3\}\cdot S$ Ions [opba = *ortho*-Phenylenebis(oxamato), S = Solvent Molecules]

Myrtil L. Kahn,[a] Marc Verelst,[b] Pierre Lecante,[b] Corine Mathonière,[a] and Olivier Kahn*[a]

Keywords: Lanthanides / WAXS / Ladder polymers / Rare-earth compounds / Supramolecular chemistry

The compounds of formula $Ln_2[M(opba)]_3\cdot xH_2O\cdot yDMSO$ containing 4f Ln^{III} and 3d M^{II} ions have been synthesized; opba stands for *ortho*-phenylenebis(oxamato). These compounds crystallize poorly, and hence structural information has been obtained from the wide angle X-ray scattering (WAXS) technique. It has been shown that the compounds present the same ladder-like motif as that previously described for $Tm_2[Cu(opba)]_3\cdot 4H_2O\cdot 10DMF$. Changing the Ln^{III} and/or M^{II} ions results in more or less pronounced distortions of the ladders. For a given M^{II} ion, changing the Ln^{III} ion from La^{III} to Lu^{III} results in a decrease of the Ln–M distance parallel to the lanthanide contraction. In the same way, for a given rare earth, changing the M^{II} ion from Cu^{II} to Ni^{II} and Zn^{II} ions also results in the decrease of the Ln–M distance in accord with the decreasing radii of the M^{II} ions. The structural details have been analyzed and discussed.

Introduction

For one decade or so, we have been concerned with the chemistry and physics of molecular compounds containing both 4f and 3d metal ions. We first focused on the $Ln^{III}-[Cu(pba)]^{2-}$ systems where Ln^{III} stands for a trivalent lanthanide ion and pba for the bisbidentate ligand 1,3-propylenebis(oxamato). Depending on the $Ln^{III}/[Cu(pba)]^{2-}$ stoichiometry and the synthetic conditions, three structures have been found, namely tube-like motifs, double sheet layers, and ladder-like motifs. Subsequently, we used the $[Cu(opba)]^{2-}$ precursor where opba stands for *ortho*-phenylenebis(oxamato). So far, one- and two-dimensional compounds have been characterized, some of them exhibiting a long-range magnetic ordering at low temperature.[1]

It is now well established that the interaction between Gd^{III} and Cu^{II} ions is ferromagnetic. On the other hand, the nature of the interaction when Gd^{III} is replaced by another magnetic Ln^{III} ion is still an open question. The presence of an orbital momentum makes the theoretical approach very difficult. Recently, we decided to tackle this problem, and to utilize a chemical approach.[2] Let us consider a compound involving both 4f Ln^{III} and 3d M^{II} magnetic ions. The magnetic behavior of such a system is governed by two factors, namely the coupling between Ln^{III} and M^{II} magnetic centres on the one hand, and the thermal population of the Stark levels of Ln^{III} on the other hand. Our approach consists of replacing the magnetic 3d M^{II} ion by a diamagnetic one, such as Zn^{II}. The magnetic behavior of a $Ln^{III}Zn^{II}$ compound is governed only by the thermal population of the Stark levels. Comparing the magnetic properties of the $Ln^{III}M^{II}$ and $Ln^{III}Zn^{II}$ compounds results in a qualitative estimation of the nature of the $Ln^{III}-M^{II}$ interaction, provided that the $Ln^{III}M^{II}$ and $Ln^{III}Zn^{II}$ compounds have similar structures.

In this paper we describe the synthesis and the structural characterization of polymeric compounds of formula $Ln_2[M(opba)]_3\cdot xH_2O\cdot yDMSO$ where M^{II} may be Cu^{II}, Ni^{II} or Zn^{II} and DMSO is dimethyl sulfoxide. Most of these compounds crystallize poorly, and we used the wide-angle X-ray scattering (WAXS) technique to obtain structural information. Even if the WAXS technique cannot give the exact structure as an X-ray diffraction study in principle does, it has been successfully utilized to structurally characterize inorganic polymers.[3] Furthermore, for one of our compounds, a structure determined from X-ray diffraction is available. This structure may be utilized as a starting guess to interpret the WAXS data for the other compounds.

Results

First Approach

Figure 1 (top) shows the reduced intensities for three selected compounds, and Figure 1 (bottom) shows the RDFs. The reduced intensity represents the structural part of the scattering phenomenon after the full correction procedure. The Fourier transform of this spectrum gives the RDF which can be considered as a histogram of ordered distances weighted by the distance multiplicity and the

[a] Laboratoire des Sciences Moléculaires, Institut de Chimie de la Matière Condensée de Bordeaux, UPR No 9048,
F-33608 Pessac, France
Fax: (internat.) + 33(0)556842649
E-mail: kahn@icmcb.u-bordeaux.fr
[b] Centre d'Elaboration de Matériaux et d'Etudes Structurales, UPR CNRS No 8011,
BP 4347, 29 rue Jeanne Marvig, F-31055 Toulouse, France

  1434–1948/99/0303–0527 $ 17.50+.50/0

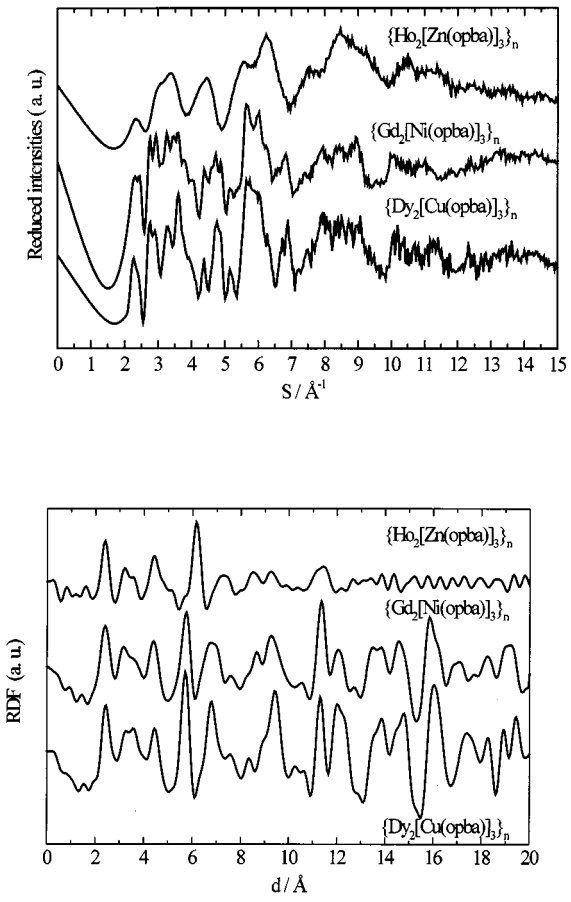

Figure 1. Overview of the experimental reduced intensities (top) and the Radial Distribution Function (RDF, bottom) for three selected samples

number of electrons engaged in these distances. Thus, an intense peak on the RDF indicates a frequent distance between two atoms.

A first qualitative look shows that the spectra are very similar to each other. The spectra of nickel- and copper-containing compounds are almost identical. The few small differences which can be detected will be discussed below. The spectra of the zinc-containing compounds differ a little bit more. This is mainly due to two factors: First, the $\{Ln_2[Zn(opba)]_3\}\cdot S$ compounds are more poorly crystallized; second, a systematic shift of each RDF peak towards longer distances is observed. The coherence length is limited to approximately 12 Å, as revealed by the collapse of ordered distances beyond this limit in the RDF of $\{Ho_2[Zn(opba)]_3\}\cdot S$.

The structures of a few oxamato-bridged $Ln^{III}Cu^{II}$ compounds were determined by X-ray diffraction on single crystals: $Gd_2[Cu(pba)]_3[Cu(H_2O)_5]\cdot 20H_2O$ presents a layered structure,[1] $Sm_2[Cu(pba)]_3\cdot 23H_2O$ shows infinite tube-like motifs,[1] and $Dy_2[Cu(pba)]_3\cdot 23H_2O$[1] and $Tm_2[Cu(opba)]_3\cdot 4H_2O\cdot 10DMF$[4] adopt a ladder-type structure. The theoretical RDFs were calculated for these three different architectures and compared to the experimental RDFs. In all cases, the best fit was obtained for the ladder-type structure. As shown in Figure 2, the uprights are made of Ln[M(opba)] units, with M = Cu, Ni or Zn, and the rungs are made of [M(opba)] units bridging Ln atoms from each upright. When seen along the direction of a rung, the two edges of the ladder are in an eclipsed conformation. Each Ln^{III} ion is surrounded by three $[M(opba)]^{2-}$ groups, its coordination sphere being completed by solvent molecules. Let us consider a specific example: $Dy_2[Cu(opba)]_3\cdot 3H_2O\cdot 9DMSO$. Figure 3 compares the experimental RDF for $Dy_2[Cu(opba)]_3\cdot 3H_2O\cdot 9DMSO$ with the RDF calculated from the X-ray diffraction data for $Tm_2[Cu(opba)]_3\cdot 4H_2O\cdot 10DMF$. The fit is fairly good up to 18 Å, which strongly suggests that $Dy_2[Cu(opba)]_3\cdot 3H_2O\cdot 9DMSO$ also has a ladder-type structure. The main difference between experimental and calculated RDFs is the shift of the peak centred at 9.85 Å in $Tm_2[Cu(opba)]_3\cdot 4H_2O\cdot 10DMF$ which is located around 9.40 Å in $Dy_2[Cu(opba)]_3\cdot 3H_2O\cdot 9DMSO$. In $Tm_2[Cu(opba)]_3\cdot 4H_2O\cdot 10DMF$ this peak corresponds to the *a* lattice parameter, i.e. to the distance between two ladders [see Figure 2 (bottom)]. Apparently, this distance is smaller in $Dy_2[Cu(opba)]_3\cdot 3H_2O\cdot 9DMSO$ than in $Tm_2[Cu(opba)]_3\cdot 4H_2O\cdot 10$ DMF, suggesting that the packing distance between two ladders is smaller in $Dy_2[Cu(opba)]_3\cdot 3H_2O\cdot 9DMSO$ than in $Tm_2[Cu(opba)]_3\cdot 4H_2O\cdot 10DMF$. This difference may be attributed to the fact that the volume of 4 H_2O and 10 DMF molecules is larger than that of 3 H_2O and 9 DMSO molecules. Beyond 18 Å the quality of the fitting decreases somewhat, but for such long distances inter-ladder packing interactions involving non-coordinated solvent molecules become important.

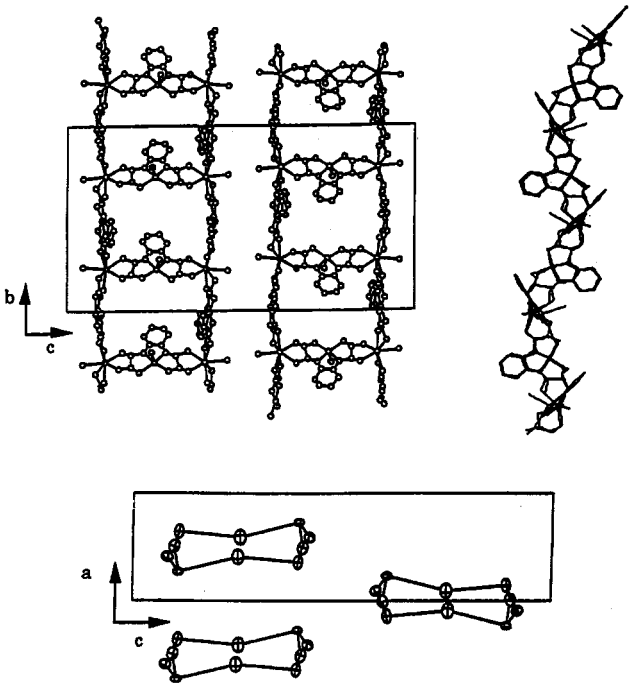

Figure 2. Structure of $Tm_2[Cu(opba)]_3\cdot 4H_2O\cdot 10DMF$ determined from X-ray diffraction; top left: view of two neighboring ladders in the *bc* plane; top right: view of one of the ladders rotated by 90°; bottom: schematic view of the ladders projected in the *ac* plane

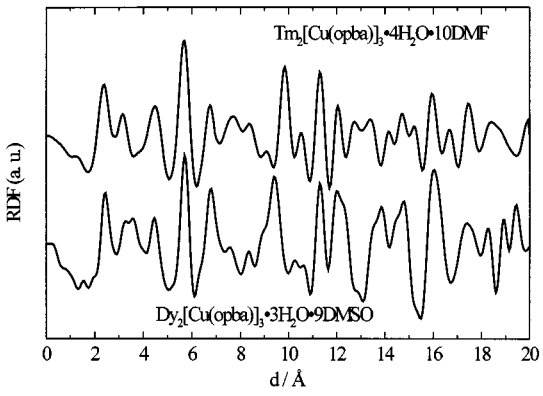

Figure 3. Comparison of the experimental RDF for $Dy_2[Cu(opba)]_3\cdot 3H_2O\cdot 9DMSO$ and the theoretical RDF for $Tm_2[Cu(opba)]_3\cdot 4H_2O\cdot 10DMF$ calculated from the structural data of ref.[4]: space group $P2_12_12_1$, a = 9.864 Å, b = 20.855 Å, c = 39.101 Å

Modeling of the $Dy_2[Cu(opba)]_3$ Ladder

Even if the structures of $Dy_2[Cu(opba)]_3\cdot 3H_2O\cdot 9DMSO$ and $Tm_2[Cu(opba)]_3\cdot 4H_2O\cdot 10$ DMF appear to be very similar, systematic shifts around 0.1 to 0.2 Å can be detected on the RDF peaks, and we decided to go further in the interpretation of the WAXS data. The starting model is a single ladder of $Tm_2[Cu(opba)]_3$ generated from crystallographic data, in which the inter-ladder contributions are obviously ignored. It follows that some slight distortions are imposed on the model in order to obtain a perfect agreement between theoretical and experimental RDF's. The final model is shown in Figure 4. Figure 5 shows the reduced intensities (top) and the RDF (bottom) computed from both experimental data and the model of Figure 4. We can notice that the Ln−Cu distances through the oxamato bridge are found to be slightly larger in $Dy_2[Cu(opba)]_3\cdot 3H_2O\cdot 9DMSO$ than in $Tm_2[Cu(opba)]_3\cdot 4H_2O\cdot 10DMF$ (Dy−Cu = 5.74 Å and Tm−Cu = 5.59 Å).

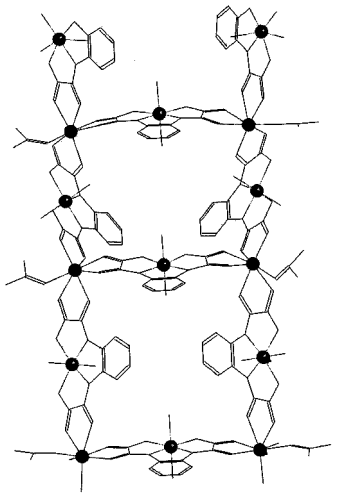

Figure 4. Structure of $Dy_2[Cu(opba)]_3\cdot 3H_2O\cdot 9DMSO$ as deduced from the WAXS study (see text); main distances: Cu−O and Cu−N: 1.95 to 2.1 Å; Dy−O: 2.27 to 2.38 Å; Dy−S: 3.55 Å; Dy−Cu: 5.72 to 5.76 Å; Dy−Dy: 11.21 to 11.36 Å

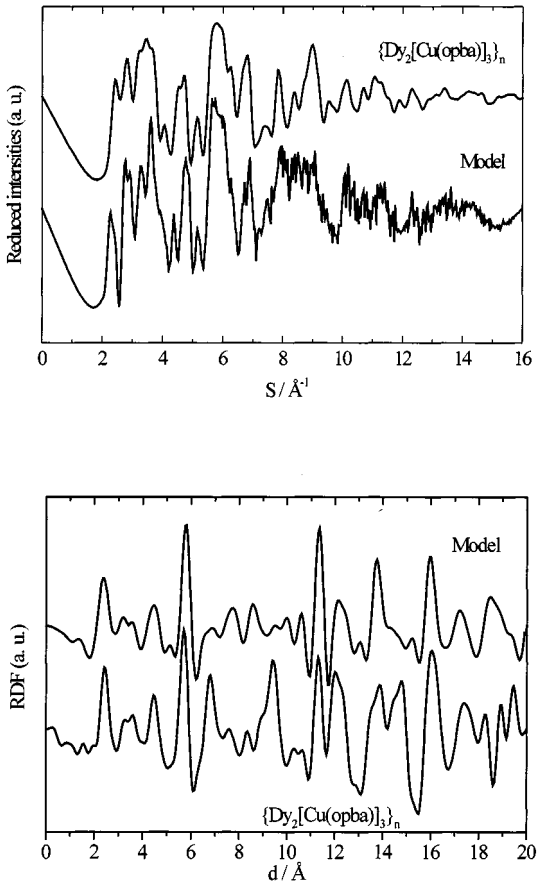

Figure 5. Reduced intensities (top) and experimental and theoretical RDFs (bottom) for $Dy_2[Cu(opba)]_3\cdot 3H_2O\cdot 9DMSO$

An interesting feature is the presence of a RDF peak centered around 3.55 Å in all the compounds containing DMSO molecules. This peak does not appear in the RDF calculated from the crystallogaphic data for $Tm_2[Cu(opba)]_3\cdot 4H_2O\cdot 10DMF$ (compare Figures 3 and 5). A simulation suggests that this distance could correspond to a Ln−S separation associated with a DMSO molecule coordinated to the Ln^{III} ion through an oxygen atom. This hypothesis is strengthened by the fact that the intensity of this peak corresponds approximately to one sulfur atom per lanthanide atom.

The agreement between experimental and calculated RDFs suggests that our model is essentially valid. However, two peaks, at 9.4 Å and 14.7 Å, are not expected in our model. These two peaks arise from intermolecular distances which are not at all modeled. Probably, the peak centred around 9.4 Å is due to the a cell parameter whereas the second one centered at 14.7 Å is the packing distance between two ladders in a same cell (see Figure 2). This hypothesis is strengthened by the fact that these two distances are equal to 9.86 Å and 14.75 Å, respectively, in $Tm_2[Cu(opba)]_3\cdot 4H_2O\cdot 10DMF$.

Ladder Distortions Induced by Metal-Ion Substitutions

Performing the modeling-distortion-fitting procedure for all the compounds would be extremely cumbersome. Such a work was carried out in one case (DyCu compound) in order to demonstrate that the compound has the ladder-type structure found for $Tm_2[Cu(opba)]_3 \cdot 4H_2O \cdot 10DMF$, with some weak distortions of the ladders. Precise assignment of the RDF peaks was also one of our goals. It is possible to determine accurately some structural characteristics such as the Ln−M (5.74 Å for the DyCu compound) and Ln−Ln (11.3 Å for the DyCu compound) distances through the opba bridge as Ln and M are changed. The results are shown in Figure 6. The two curves of Figure 6 confirm that the nickel- and copper-containing compounds have very similar structures. For a same Ln^{III} ion, the width of the ladders is slightly smaller in the copper derivatives, which is in line with the difference in ionic radius between Cu^{II} and Ni^{II} (0.72 and 0.78 Å, respectively). The width of the ladders is even larger in the zinc derivatives, in agreement with an ionic radius of 0.83 Å for Zn^{II}. In a similar way, for a same M^{II} ion the width of the ladders decreases as the atomic number of Ln increases. This observation is obviously in line with the contraction of the atomic radius from the left to the right of the lanthanide series, from 1.22 Å for La^{III} to 0.85 Å for Lu^{III}. It can be noticed that in the LnZn series two compounds, GdZn and TbZn, show larger Ln−Ln distances, 11.65 and 11.75 Å, respectively, than those for the other LnZn compounds (11.45 Å in average). This might result from the relative flexibility of the Ln−Zn−Ln alignment, i.e. the deviation of ρ (the angle between the two Ln−Zn bonds) from 180° (see below).

To obtain further information on the linearity of the Ln−[M(opba)]−Ln network in the various compounds, we calculated the ratios of the distances, ρ = Ln−Ln/Ln−M. If this network is strictly planar, ρ should be equal to 2; a ρ value smaller than 2 reveals a distortion of the network. For the compounds with M = Ni and Cu, ρ is in the range 1.96−1.98, i.e. very close to 2. On the other hand, for the compounds with M = Zn, ρ ranges between 1.80 and 1.85. Probably, the ladders in the zinc-containing compounds are more distorted than in the nickel- and copper-containing derivatives. However, as shown in Figure 6, two compounds of the Zn series (GdZn and TbZn) seem to deviate from linearity less than the other compounds of this series. In any case, this distortion would explain why the zinc derivatives are less crystalline than the nickel and copper ones. In these zinc compounds, this distortion probably induces a statistical disorder which reduces the coherence length to about 12 Å.

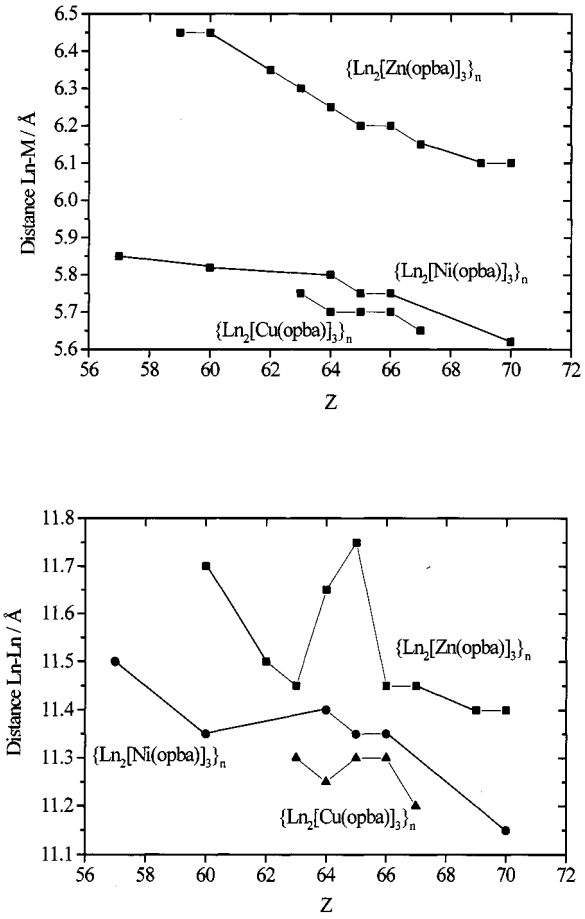

Figure 6. Evolution of M−Ln (top) and Ln−Ln (bottom) distances as a function of the atomic number of the Ln and M elements

Conclusion

This WAXS study on a new series of 4f−3d compounds proves without doubt that all the $\{Ln_2[M(opba)]_3\} \cdot S$ compounds have similar structures. These compounds crystallize poorly. However, the coherence length is important enough to strongly suggest that the structures consist of ladder-like motifs, very similar to those found in $Tm_2[Cu(opba)]_3 \cdot 4H_2O \cdot 10DMF$. These WAXS studies allow us not only to confirm the ladder-type structure but also to determine precisely important distances such as Ln−M, Ln−Ln and Ln−S. The Ln−M separations across the oxamato bridge range from 5.60 to 6.45 Å, and the separation between two Ln^{III} ions connected in the transverse direction range from 11.15 to 11.75 Å depending on the nature of the Ln^{III} and M^{II} ions. The packing distances between two ladders range from 9.0 to 9.5 Å (*a* lattice parameter) and is around 14.7 Å between two ladders in the same cell. For a given M^{II} ion, changing Ln^{III} from La^{III} to Lu^{III} ion results in the decrease of the Ln−M distance in accord with the lanthanide contraction. In the same way, for a given rare earth, changing the M^{II} ion from Cu^{II} to Ni^{II}, and then Zn^{II} results also in the decrease of the Ln−M distance in accord with the decreasing radii of the M^{II} ions. These studies confirm that the determination of the structure of polymeric compounds is possible with the WAXS technique and that precise structural information can be obtained.

Systematic magnetic measurements are in progress and will be published in a subsequent paper. This structural

study was a prerequisite to discussing and interpreting the magnetic data.

Experimental Section

Syntheses. – Starting Materials: $Ln(NO_3)_3\cdot xH_2O$,[5] Et_2H_2opba and $(NMe_4)_2[Cu(opba)]$,[6] were synthesized according to described procedures. The Zn^{II} precursor, $(NBu_4)_2[Zn(opba)]$, was synthesized as follows: A solution of Et_2H_2opba (1.545 g, 5 mmol) and NBu_4OH (2.62 ml, 40 wt.-% sol. in water, 4 mmol) in MeOH was stirred at 60°C for 30 min. A methanolic solution of $Zn(Ac)_2\cdot 2H_2O$ (0.219 g, 1 mmol) was added dropwise. A white precipitate was immediately formed. The solid was collected by centrifugation of the mixture, washed three times with MeOH and dried under vacuum (2.8 g, yield 70%). – ^{1}H NMR [D$_6$]DMSO: δ = 7.94 (br. s, 2 H, *aromatic*); 6.57 (br. s, 2 H, *aromatic*); 3.16, 1.55, 1.29 [3 br. m, 48 H, $N(CH_2)_3CH_3$]; 0.91 (br. m, 24 H, CH_3). – IR (principal vibrations; KBr; cm^{-1}): $\tilde{\nu}$ = 2961.7 (w), 2874.0 (w): ν(C–H); 1598.1 (s), 1572.5 (s): ν(C=O); 753.5 (w): aromatic ring. – $C_{42}H_{96}N_4O_{16}Zn$ (978.6): calcd. C 51.5, H 9.9, N 5.7, Zn 6.7; found C 50.8, H 8.9, N 5.4, Zn 7.3.

Ni^{II} Precursor $(NMe_4)_2[Ni(opba)]$: A solution of Et_2H_2opba (1.545 g, 5 mmol) and NMe_4OH (7.18 ml, 25 wt.-% sol. in water, 20 mmol) in MeOH was stirred at 60°C for 30 min. A methanolic solution of $Ni(ClO_4)_2\cdot 6H_2O$ (1.828 g, 5 mmol) was added dropwise. The solution was filtered and the solvent was removed. The addition of a small amount of distilled MeOH gave a precipitate of $(NMe_4)(ClO_4)$. The reaction mixture was then kept at –18°C for 12 h, then filtered. The solvent was removed under reduced pressure to give an orange oil which crystallized by addition of diethyl ether (3.4 g, yield 85%). – ^{1}H NMR ([D$_6$]DMSO): δ = 7.80 (br. s, 2 H, *aromatic*); 6.55 (br. s, 2 H, *aromatic*); 3.10 (s, 24 H,CH_3). – IR (principal vibrations; KBr; cm^{-1}): $\tilde{\nu}$ = 3018.9 (w): ν(C–H); 1663.8 (s), 1636.1 (s): ν(C=O); 618.5 (w) aromatic. – $C_{22}H_{44}N_4NiO_{10}$ (583.3): calcd. C 45.3, H 7.6, N 9.6, Ni 10.0; found C 45.6, H 7.1, N 11.8, Ni 9.6.

$\{Ln_2[M(opba)]_3\}\cdot S$: All the $\{Ln_2[M(opba)]_3\}\cdot S$ compounds were synthesized by using the same general procedure. Here is described the general procedure. A solution of $Ln(NO_3)_3\cdot xH_2O$ (33 mmol), dissolved in 5 mL of DMSO, was added dropwise to a solution of $(Cat^+)_2[M(opba)]$ (50 mmol), dissolved in 10 mL of DMSO solution. A precipitate was formed and the mixture was stirred for 3 h. The solid was collected by centrifugation, washed three times with DMSO and three times with ether, then dried under vacuum. – IR (principal vibrations; KBr; cm^{-1}): $\tilde{\nu}$ = $\{Dy_2[Cu(opba)]_3\}\cdot S$: 1626.4 (s), 1596.1 (s), 1572.5 (s): ν(C=O); 1014.5 (s), 951.1 (m): ν(S=O). $\{Ho_2[Zn(opba)]_3\}\cdot S$: 1590.4 (s), 1560.4 (s): ν(C=O); 1016.8 (s), 954.3 (m) ν(S=O). $\{Gd_2[Ni(opba)]_3\}\cdot S$: 1618.0 (s), 1572.5 (s): ν(C=O); 1014.8 (s), 953.0 (m): ν(S=O). – $C_{48}H_{72}Cu_3Dy_2N_6O_{30}S_9$ (2017.3): calcd C 28.6, H 3.6, Cu 9.4, N 4.2, S 14.3; found C 28.3, H 2.8, Cu 8.5, N 5.8, S 14.5; $C_{31}H_{45}Gd_2N_6Ni_3O_{33.5}S_{0.5}$ (1544.3): calcd C 24.1, H 2.9, Gd 20.4, N 5.4, S 1.0, Ni 11.4; found C 25.3, H 2.9, Gd 20.0, N 5.3, S 0.4, Ni 10.5; $C_{44}H_{64}Ho_2N_6O_{30}S_7Zn_3$ (1907.5): calcd C 27.7, H 3.4, Ho 17.3, N 4.4, S 11.8; found C 29.6, H 3.9, Ho 17.4, N 4.3, S 11.7.

WAXS Studies: A typical experiment was performed as follows: The sample was sealed in a Lindeman capillary. The diffusion spectrum scattered by the sample irradiated with graphite-monochromatized molybdenum K_α radiation (λ = 0.71069 Å) was obtained using a LASIP diffractometer.[7] 457 intensities corresponding to equidistant points [$s = 4\pi(\sin\theta/\lambda)$; Δs = 0.035 Å^{-1}] were collected in the 0° < θ < 65° range. Measurements of air and Lindeman capillary diffusion were carried out exactly under the same conditions. The raw sample scattered intensity (sample + air + capillary) was corrected for air and capillary contributions by spectra subtraction taking into account absorption from sample, then corrected for polarization and self absorption effects. Normalization was performed using Norman and Krogh-Moe's method.[8] The atomic scattering factors were taken from Cromer and Waber.[9] The reduced experimental Radial Distribution Function (RDF) was calculated similarly as described in ref.[10] Theoretical structural models were built up using the CERIUS2 program.[11] The theoretical RDF was computed from the structural models by Fourier transform of the theoretical intensities calculated according to the Debye formula[12] using the KURVLR program.[13] Debye–Waller factors commonly observed in related crystalline structures were used for the computation.

[1] O. Guillou, O. Kahn, R. L. Oushoorn, K. Boubekeur, P. Batail, *Inorg. Chim. Acta* **1992**, *198–200*, 119–131.
[2] M. L. Kahn, C. Mathonière, O. K ahn, *International Conference on f Elements*, September 14–18, **1997**, Paris, France.
[3] M. Verelst, L. Sommier, P. Lecante, A. Mosset, O. Kahn, *Chem. Mater.* **1998**, *10*, 980.
[4] R. L. Oushoorn, K. Boubekeur, P. Batail, O. Guillou, O. Kahn, *Bull. Soc. Chim. Fr.* **1996**, *133*, 777.
[5] J.-C. G. Bünzli, G. R.Choppin, *Lanthanide Probes in Life, Chemical and Earth Sciences*, Elsevier, Amsterdam, The Netherlands, **1989**.
[6] H. O. Stumpf, Y. Pei, O. Kahn, J. Sletten, J.-P. Renard, *J. Am. Chem. Soc.* **1993**, *115*, 6738.
[7] The LASIP diffractometer has a geometry especially set up for scattering measurements. It minimizes every external parasite scattering phenomenon.
[8] [8a] N. Norman, *Acta Crystallogr.* **1957**, *10*, 370. – [8b] Krogh-Moe, *Acta. Crystallogr.* **1956**, *9*, 951.
[9] D. Cromer, T. Waber, *J. International Tables for X-ray Crystallography*: Kynoch Press, Birmingham, **1974**, vol. 4.
[10] See for example: [10a] A. Mosset, P. Lecante, J. Galy, *J. Phil. Mag. B* **1982**, *46*, 137. – [10b] A. Burian, P. Lecante, A. Mosset, J. Galy, *J. Non-Crystalline Solids* **1987**, *90*, 633. – [10c] C. Laberty, M. Verelst, P. Lecante, A. Mosset, P. Alphonse, A. Rousset, *J. Solid-State Chem.* **1997**, *129*, 271–276. – [10d] M. Verelst, L. Sommier, P. Lecante, A. Mosset, O. Kahn, *Chem. Mater.* **1998**, *10*, 980.
[11] CERIUS2 molecular simulation program is supplied by BIOSYM technologies and runs on an Indy Silicon Graphics workstation.
[12] P. Debye, *Ann. Physik (Leipzig)* **1915**, *46*, 809.
[13] G. Johansson, M. Sandström, *Chem. Scr.* **1973**, *4*, 195.

Received October 9, 1998
[I98346]